

Morphologies of Sol–Gel Derived Thin Films of ZnO Using Different Precursor Materials and their Nanostructures

Harish Bahadur · A. K. Srivastava ·
R. K. Sharma · Sudhir Chandra

Received: 14 June 2007 / Accepted: 14 August 2007 / Published online: 9 September 2007
© to the authors 2007

Abstract We have shown that the morphological features of the sol–gel derived thin films of ZnO depend strongly on the choice of the precursor materials. In particular, we have used zinc nitrate and zinc acetate as the precursor materials. While the films using zinc acetate showed a smoother topography, those prepared by using zinc nitrate exhibited dendritic character. Both types of films were found to be crystalline in nature. The crystallite dimensions were confined to the nanoscale. The crystallite size of the nanograins in the zinc nitrate derived films has been found to be smaller than the films grown by using zinc acetate as the precursor material. Selected area electron diffraction patterns in the case of both the precursor material has shown the presence of different rings corresponding to different planes of hexagonal ZnO crystal structure. The results have been discussed in terms of the fundamental considerations and basic chemistry governing the growth kinetics of these sol–gel derived ZnO films with both the precursor materials.

Keywords ZnO thin films · Morphologies · Sol–Gel · XRD · SEM · TEM

Introduction

ZnO is one of the most important nanomaterials for integration in microsystems and biotechnology. It is a semiconductor with a wide band gap of 3.37 eV and large exciton binding energy of 60 meV. This makes it useful in a number of photonic applications. Due to its non-centrosymmetric characteristics, it is piezoelectric and is used in electromechanical coupled sensors and transducers. Thin films of zinc oxide have a large number of technological applications including a variety of sensors. The preparation of ZnO thin films has been the subject of continuous research for a long time because the properties of ZnO films depend upon the method of preparation. Currently, there is a great interest in the methods of creating nanostructures on surfaces by various self-organizing techniques. These nanostructures form the basis of nanotechnology applications in sensors and molecular electronics for next generation high performance nano-devices. ZnO exist in a variety of nanostructures [1] and is expected to be the next most important nanomaterial after the carbon nanotubes.

In the present communication, we shall show that the morphological features of the sol–gel derived thin films of ZnO depend strongly on the choice of the precursor materials. Sol–gel technique of film preparation is a low-cost process and is attractive as the film properties can be tailored conveniently for a given application. The process thus becomes a preferred option over the expensive techniques such as MBE, MOCVD etc to synthesize materials for exploratory studies. A large number of candidate materials, which require screening for their compositions and properties prior to their applications in devices, can be produced at low cost using the sol–gel process. In general, zinc acetate is the precursor material for preparation of ZnO films using sol–gel process or spray pyrolysis

H. Bahadur (✉) · A. K. Srivastava · R. K. Sharma
National Physical Laboratory, K.S. Krishnan Road, New Delhi
110012, India
e-mail: hbahadur@yahoo.com

S. Chandra
Center for Applied Research in Electronics, Indian Institute of
Technology, Hauz Khas, New Delhi 110016, India

techniques [2–5]. However, zinc nitrate has also been used for preparation of nanosized zinc oxide powder. For example, Liu et al. [6] have described the formation of ordered porous ZnO film using zinc nitrate by electro-deposition method using polystyrene array templates. Studenikin et al. [7] describe the formation of undoped ZnO film by spray pyrolysis of zinc nitrate solution at high temperature. Zinc nitrate is also used for the synthesis of ZnO nanoparticles [8]. Micropatterns of ZnO have been synthesized [9] on photocatalytically activated regions of TiO₂ in an aqueous solution of zinc nitrate and dimethylamine-borane by an electroless deposition process. The as-deposited ZnO micropatterns showed a polycrystalline wurtzite structure. There are several reports [6–8] in which ZnO has been grown using zinc nitrate as the starting material. However, most of the papers reported involve either spray pyrolysis using a solution of zinc nitrate or electrodeposition process.

Our earlier work [10–15] has shown that the films grown by zinc acetate and zinc nitrate as precursor materials show different morphological features. Films grown by zinc nitrate show a rapid and random crystallization than the films grown by zinc acetate. A smoother topography is obtained for the films grown by using zinc acetate than for the films grown by zinc nitrate. Scanning tunneling microscopy showed that the films grown by zinc acetate as precursor were uniform. Nano-structured ZnO grains of size ranging from 20 to 60 nm were obtained on the film grown by sol–gel spin process using zinc nitrate as precursor material on a quartz substrate. Individual grains showed a sharp contrast with different facets and boundaries. In this paper, we shall present our results and extend a discussion in terms of basic chemical reactions giving our reasoning to the observed morphologies. We shall describe and discuss the results separately for the two types of precursor materials used. For a ready reference and coherent discussion, some of the micrographs will be reproduced from the previous papers [10–15].

Experimental

The films were grown by sol–gel technique on silicon and fused quartz substrates. The reason for choosing two types of substrates, silicon and quartz, was to check the dependency of morphological features whether they are characteristics of sol or substrates. The sols were prepared by using two different routes and precursor materials viz. zinc nitrate and zinc acetate. Accordingly, the solvent chosen were also different. The reason for using two different solvents was due to the fact that the solubility of two precursor materials zinc nitrate and zinc acetate is different in their solvents. While zinc nitrate was dissolved in

ethylene glycol monomethyl ether, zinc acetate was dissolved in isopropyl alcohol. Both the sols were made to have sufficient amount of the precursor material dissolved under the limit of equilibrium reaction. It may be mentioned here that all chemicals used were procured from E.Merck (Germany) and were of AR grade.

The growth procedure consisted of first making the surface of the silicon substrate hydrophilic by boiling the Si wafer in 70% HNO₃ followed by rinsing in de-ionized water and subsequent drying. This process oxidizes the Si surface to SiOH and improves its adhesion. The sol was prepared by two different routes. The first route involved dissolving 10 g of zinc nitrate [Zn(NO₃)₂ · 6H₂O] in 100 mL of ethylene glycol monomethyl ether [CH₃O–CH₂–CH₂OH] to form the zinc solution. The other route of sol preparation was to prepare 10% solution of zinc acetate [Zn(CH₃COO)₂ · 2H₂O] by dissolving 10 g of zinc acetate in 100 mL of boiling isopropyl alcohol at 84 °C. This was followed by clarifying the turbid solution by adding a few drops of diethanolamine. For the film preparation, a Si wafer was mounted on a spinner and the sol was placed on top of it and the wafer was allowed to spin at the rate of 3000 rpm. This step was followed by drying the coated wafer at 100 °C and subsequent baking at 450 °C for one hour. Films were prepared using both the routes one by one. Multiple coatings were done to obtain the workable thickness of the film using both the routes of sol preparation. The ellipsometric data show that for ten coatings, the film thickness was only of the order of 2000–2500 Å. Bright field high magnification micrographs were recorded by using a transmission electron microscope (TEM model JEOL JEM 200Cx) operated at 200 kV to investigate the different morphologies observed under SEM.

Results and Discussion

It may be mentioned here that visually the films appeared continuous and uniform and blue in color.¹ However, when examined under scanning electron microscope, in general,

¹ The blue color corresponds to the difference in the refractive index between the material (ZnO on Si substrate) and the air. For a high-index material such as Si, the surface reflection is about 35% of the incident light in an air environment. For the minimum reflection, the index of coating must satisfy the condition

$$n_c = (n_1 n_2)^{1/2} \quad (1)$$

where n_c , n_1 , n_2 are the refractive indices of coating, medium and substrate, respectively. The thickness of the coated film is then determined by the equation

$$t_c = \lambda_0 / 4n_c \quad (2)$$

where λ_0 is the wavelength where zero reflectivity is desired.

the films grown by using two different precursor material showed different kinds of morphologies. Having observed the difference in the morphologies, we have investigated the nature of products formed when zinc nitrate and zinc acetate were subjected to different conditions of hydrolysis. In the case of zinc nitrate, it was observed that pure zinc nitrate is recovered unchanged even after boiling for two hours whereas zinc acetate always give basic zinc acetate or zinc hydroxide depending upon the time of boiling. These results were confirmed by infrared absorption measurements and will be described elsewhere.

Zinc Nitrate as the Precursor Material

The SEM examination of the films revealed that the films grown by using zinc nitrate exhibited dendritic character with agglomeration of dendrites. As an example, the set of micrographs in Fig. 1 depict the general character of morphological features as revealed by SEM (model LEO-0440 equipped with ISIS 300 Oxford microanalysis system EDS attachment) for the ZnO film grown on a Si substrate by using zinc nitrate as the precursor material. From the micrographs, it appears that the films are patchy and not continuous. There are dendrites with agglomeration in

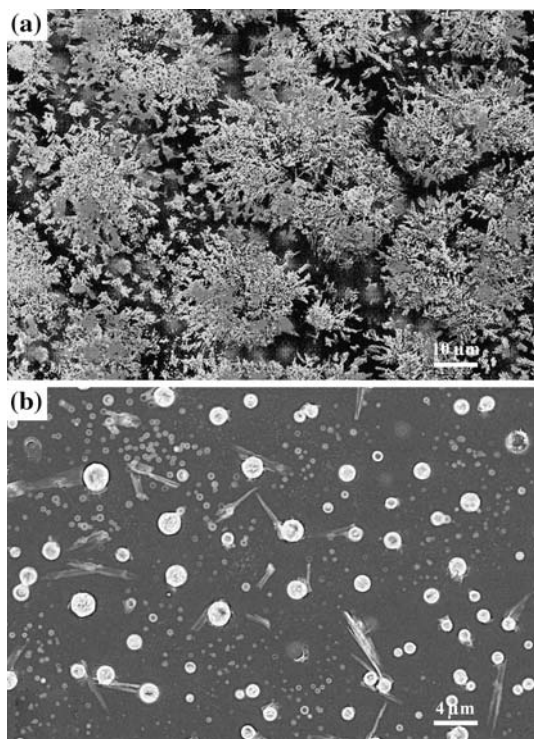


Fig. 1 A set of SEM micrographs showing the dendritic character of morphological features of the ZnO thin film grown on Si substrate by sol-gel spin process using zinc nitrate as the precursor material. Micrographs (a), and (b) are drawn from Refs. [14, 15]

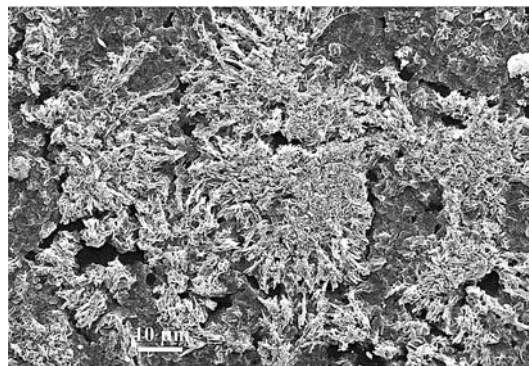


Fig. 2 SEM micrograph showing the dendritic character of morphological features of the ZnO thin film grown on quartz substrate by sol-gel spin process using zinc nitrate as the precursor material

certain areas on the film. This nature of morphology was typical of using zinc nitrate as the starting material. However, as mentioned earlier, visually the films appeared continuous, smooth and shining. We have investigated the effect of substrate other than Si. The other substrate was a fused quartz. As an illustration, Fig. 2 depicts a micrograph on quartz substrates. It may be noted that in this case also, the film does not appear to be continuous but has the dendritic character. This dendritic character is thus typical of using zinc nitrate as the precursor material. From the micrographs shown in Figs. 1 and 2, it appears from the nature of the dendrites that the crystallite formation occurs randomly as well as rapidly. These dendrites were found to be crystalline in nature [13].

Figure 3 represents the EDS spectrum for the ZnO film on Si substrate of micrograph shown in Fig. 1(b). The strong peak of Si at 1.8 eV is that of the signal coming from the substrate because the film thickness was lower

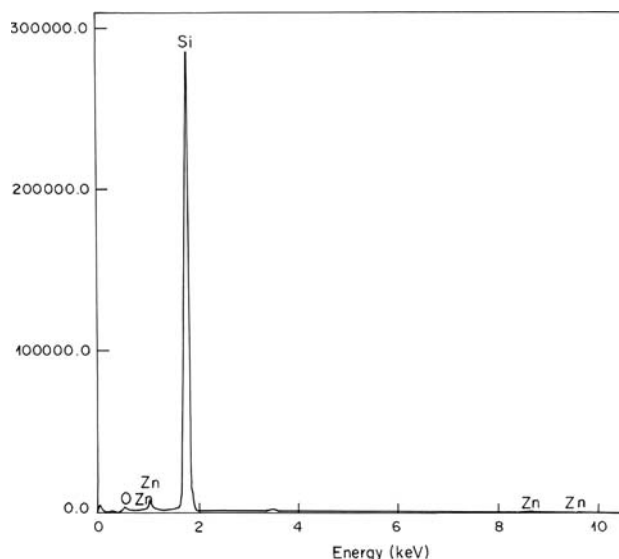


Fig. 3 EDS spectrum of ZnO thin film grown on Si substrate by sol-gel spin process using zinc nitrate as the precursor material

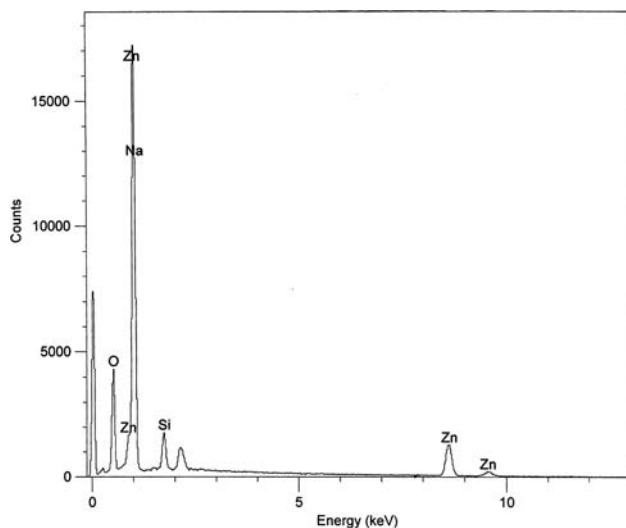


Fig. 4 EDS spectrum of ZnO thin film grown on quartz substrate by sol–gel spin process using zinc nitrate as the precursor material

than the penetration depth of the incident electron of 15 keV. The main lines $ZnK\alpha$ (8.64 keV) and $ZnK\beta$ (9.57 keV) are also not observable due to the small thickness of film. Figure 4 represents the EDS spectrum for the ZnO film grown on quartz substrate. In this spectrum, $ZnK\alpha$ and $ZnK\beta$ lines are clearly observable. The peak for oxygen is also clearly seen.

Figure 5 depicts a TEM bright field micrograph on a Si substrate using zinc nitrate precursor. The individual grains show a distinguished contrast on the surface. In some cases, different facets with sharp edges may also be seen. The faceted morphology of these grains should be linked to the crystallographic symmetry of the wurtzite ZnO and a preferred growth direction during deposition. The micrograph shows that the film is polycrystalline in nature with a random distribution of nano-grained ZnO in it. The electron diffraction pattern shows only the 103 and 002 planes. Some other important reflections such as 110, 102 and 101

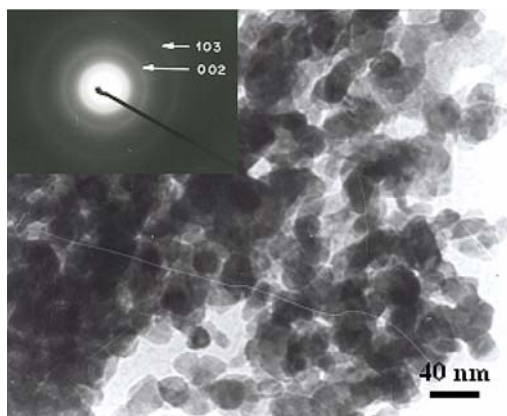
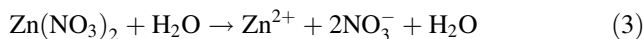


Fig. 5 Bright field TEM micrograph of the nanograins of ZnO grown by zinc nitrate. Electron diffraction is shown in the inset

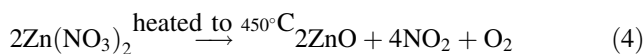
which were obtained in the case of use of zinc acetate (Fig. 8 shown later) may be noticed to be missing in Fig. 5. The absence of the later planes (110, 102 and 101) elucidates that the film has certain texture with preferred growth direction of 103 and 002 planes.

Reaction Mechanism of Film Deposition Zinc Nitrate as the Precursor Material

It is known that zinc nitrate is a salt of amphoteric zinc oxide and nitric acid [16–19]. On dissolving in water, zinc nitrate gets ionized to give zinc and nitrate ions as illustrated below;



The solution, on evaporation of water, gives zinc nitrate without any decomposition. This on heating gives rise to ZnO in the form of small crystallites with the evolution of NO_2 . This is illustrated below:



Such crystallites are formed rapidly in random directions and thus give rise to dendrites or island type morphology of the film structure as shown in the set of micrographs in Fig. 1. The exact nature of morphology like dendrites or island, needles etc would depend upon several parameters such as the spin speed, sol concentration, annealing temperature etc. The EDS spectra shown in Figs. 3 and 4 prominently display the peaks of Zn and O. The crystalline nature of the film was shown by selected area electron diffraction pattern (inset of Fig. 5) and also by the XRD investigations [13] revealing different crystal planes without any preferred orientation.

Zinc Acetate as the Precursor Material

Figure 6 depicts a typical micrograph obtained for the ZnO film by using zinc acetate as the precursor material. The difference in the morphological features in Fig. 6 may clearly be noticed from those shown in Figs. 1 and 2. In the case of use of zinc acetate as the precursor material the morphology of the film is very smooth with no dendrites being formed. In contrast, Fig. 6 does not show any such features, instead the film is quite smooth. Figure 7 depicts the EDS spectrum for the film grown by zinc acetate. Again, the spectrum shows that the film is primarily consisted of ZnO. $ZnK\alpha$ and $ZnK\beta$ lines are also seen in weak strength due to the small thickness of the film. The Si peak shows the signal coming from the substrate.

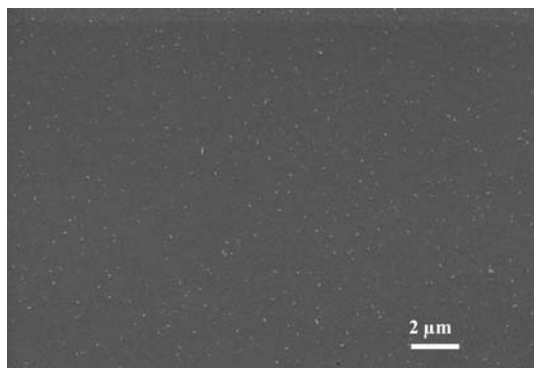


Fig. 6 SEM micrograph showing the smooth character of morphological features of the ZnO thin film grown on Si substrate by sol-gel spin process using zinc acetate as the precursor material

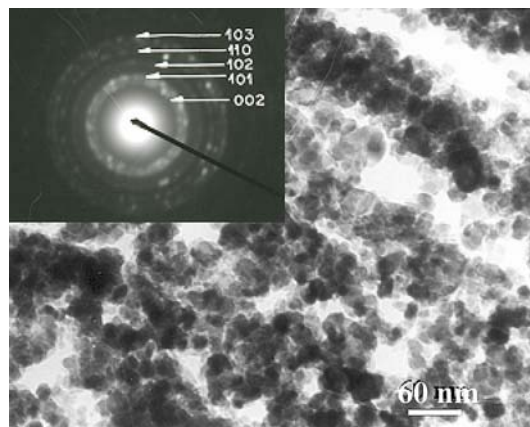


Fig. 8 Bright field TEM micrograph of the nanograins of ZnO grown by zinc acetate. Electron diffraction is shown in the inset

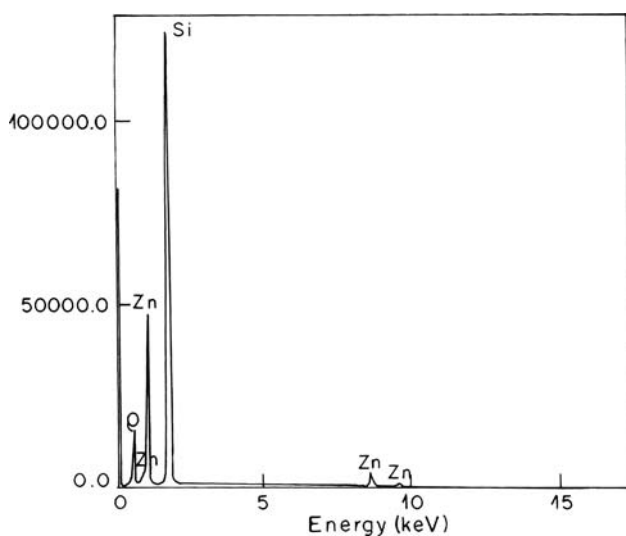


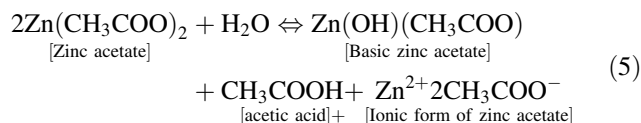
Fig. 7 EDS spectrum of ZnO thin film grown on Si substrate by sol-gel spin process using zinc acetate as the precursor material

The films were found to be crystalline in nature as seen by the X-ray diffraction pattern for the film of which the micrograph is shown in Fig. 6 [20]. The diffractogram showed in this case some degree of preferential growth in 101 direction. A representative bright field TEM micrograph (Fig. 8) for the film of which the SEM micrograph and EDS are shown in Figs. 6 and 7 shows that the distribution of grains is more or less similar to that shown in Fig. 5 for the zinc nitrate case.

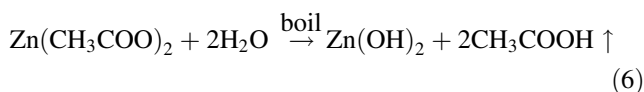
Reaction Mechanism of Film Deposition Using Zinc Acetate as the Precursor Material

Zinc acetate is a salt of amphoteric zinc oxide and a weak acid like acetic acid [16–19]. On dissolving in water, zinc acetate is partially hydrolyzed and the rest is ionized. The

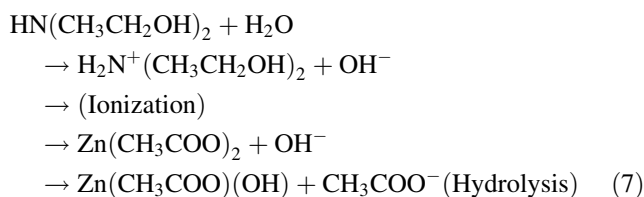
extent of hydrolysis depends upon the water available from the ambient atmospheric humidity. The hydrolysis of zinc acetate results in the formation of the basic zinc acetate, which on evaporation of the water, does not give pure zinc acetate but produces a mixture of zinc acetate and basic zinc acetate. This process is demonstrated as below;



If zinc acetate solution is boiled continuously for several hours, acetic acid and water will evaporate off and only pure basic zinc hydroxide is left behind in the process. The process of formation of zinc hydroxide by continuously boiling zinc acetate solution may be written as follows;

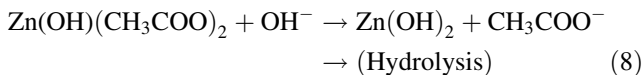


We have added a few drops of diethanaloamine to clarify the turbid solution of zinc acetate. It may be mentioned here that in the presence of amine the effect of hydrolysis of zinc acetate or basic zinc acetate becomes more pronounced as illustrated below

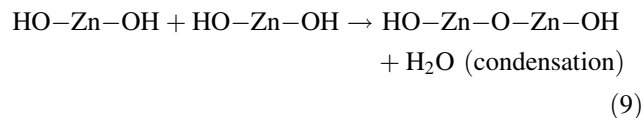


The process of formation of ZnO films using zinc acetate or basic zinc acetate precursor is illustrated below which proceeds via the process of hydrolysis, condensation

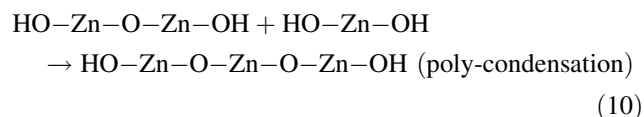
and poly-condensation. The reaction is illustrated as follows;



If two molecules of Zn(OH)_2 condense, the reaction can be expressed as;



If three molecules of Zn(OH)_2 condense, the reaction would be expressed as;



The process would continue. After the evaporation of the water molecules, this would result in a final product which can be written as $\text{HO-(Zn-O-Zn)}_n\text{-OH}$ where n is the number of molecules taking part in the condensation process (poly-condensation). Since during the course of poly-condensation, the reaction proceeds uniformly in all directions in the plane of the substrate, the process of crystallization becomes steady and thus uniform. Therefore, the reaction mechanism leads to formation of an in-plane flat film of ZnO as opposed to the case of use of zinc nitrate as the precursor material where the crystallization was rapid and random. Because of these basic differences, the crystallite size was different with the use of different precursor materials. In the case of use of zinc nitrate, the crystallite were smaller in size in comparison with those obtained by the use of zinc acetate. Below, we describe the measurement of crystallite size.

The crystallite size was estimated for both the types of films by using Scherrer formula [21]

$$D = k\lambda/\beta \cos \theta \quad (11)$$

where D is the crystallite size, k is a proportionality constant ($= 0.9$), λ is the wavelength of the X-ray radiation used ($\text{CuK}\alpha$ in the present case), β is the full width at half maximum (FWHM) of the diffraction peak (in radians) and θ is of course the Bragg angle. The $\text{CuK}\alpha$ line has the average wavelength of 1.54178 \AA and consists of two lines $\text{CuK}\alpha_1$ and $\text{CuK}\alpha_2$ with $\text{CuK}\alpha_1$ at 1.5405 \AA with a shoulder band of $\text{CuK}\alpha_2$ at 1.54433 \AA . For calculating FWHM and the crystallite size, the standard practice is to take only $\text{CuK}\alpha_1$ into consideration. Intense diffraction peaks

corresponding to the crystal planes 100, 002, 101, 102, 110, 103 and 112 were selected, and after separating out $\text{K}\alpha_2$ from $\text{K}\alpha_1$ for all the reflections for the calculation of FWHM was calculated. The crystallite size was calculated by using the Scherrer formula of Eq. (9). Presently, in our system, Bruker AXS D8 Advance diffractometer, all this exercise is done by the inbuilt $\text{Diffrac}^{\text{plus}}$ software. The crystallite size for the film grown by using zinc acetate on Si substrate was estimated to be about 25 nm in the a -axis and about 15–20 nm in the c -axis direction of the lattice. For the film grown by using zinc nitrate on Si substrate, the crystallite size obtained in the c -axis direction was in the range of 15 nm and the a -axis direction it was about 12 nm. Thus, the film prepared using zinc acetate precursor have larger crystalline size as compared to those prepared using zinc nitrate precursor. Unit cell parameters were calculated from the diffraction data by minimizing the sum of the squares of residuals of 2θ . The calculated values for zinc nitrate precursor film are: $a = 0.3255(0.0004) \text{ nm}$ and $c = 0.529(0.0008) \text{ nm}$ and for the zinc acetate precursor film are $a = 0.3255(0.0004) \text{ nm}$ and $c = 0.5216 (0.0008) \text{ nm}$. It may be noted that these values are quite close to the reported data (PDF#36-1451): $a_0 = 0.3250 \text{ nm}$ and $c_0 = 0.5207 \text{ nm}$. The electron diffraction pattern (inset of Fig. 8) demonstrated three important planes of hexagonal structure (002,101,102,110,103) in the form of continuous rings in the reciprocal space. It shows that the film is polycrystalline in nature with a random distribution of nano-grained ZnO in it. The electron diffraction pattern elucidates that the film has certain texture with preferred growth direction.

Conclusion

Experimental results on differences in the morphological features in these films grown by spin process using the two precursor materials have been presented. The present work has shown that the films of ZnO prepared by using zinc nitrate exhibit dendrites while those using zinc acetate are uniform and smooth. Explanations have been offered involving basic chemical processes in the preparation of two types of sols used for growing such films. Zinc nitrate first crystallizes in the form of small crystallites of zinc nitrate followed by decomposition on heating to give small crystallites of zinc oxide. On the other hand, zinc acetate first hydrolyzes followed by the process of condensation, poly-condensation and finally give smooth films of zinc oxide on heating at $450 \text{ }^\circ\text{C}$. The micrographs suggest that the film prepared by using zinc nitrate show a rapid and random crystallization compared to that using zinc acetate as the precursor materials.

Acknowledgments This work was done under a joint collaborative program between National Physical Laboratory (NPL) and Indian Institute of Technology, Delhi. The authors thank Mr. K. N. Sood for the SEM related investigations. The authors also express their thankfulness and appreciation to Dr. Vikram Kumar, the Director, NPL for his encouragement in the work.

References

1. Z.L. Wang, *J. Phys.: Condes. Matter* **16**, R829–R858. (Topical Review). Institute of Physics Publishing, UK (2004)
2. J.S. Kim, H.A. Marzouk, P.J. Reucroft, C.M. Hamrin, *Thin Solid Films* **217**, 133 (1992)
3. R. Kaur, A.V. Singh, R.M. Mehra, *Mater. Sci. Poland* **22**, 201 (2004)
4. M.N. Kamlasanan, S. Chandra, *Thin Solid Films* **288**, 112 (1996)
5. T. Saeed, P. O'Brien, *Thin Solid Films* **271**, 35 (1995)
6. Z. Liu, Z. Jin, J. Qiu, X. Liu, W. Wu, W. Li, *Semicond. Sci. Tech. IoP J.* **21**, 60 (2006)
7. S.A. Studenikin, N. Golego, M. Cocivera, *J. Appl. Phys.* **84**, 2287 (1998)
8. T. Yoshida, H. Minoura, *Adv. Mater.* **12**, 1219 (2000)
9. J.Y. Kim, C.H. Noh, K.Y. Song, S.H. Cho, M. Kim, J.M. Kim, *Electrochem. Solid State Lett.* **8**, H-75 (2005)
10. H. Bahadur, R. Kishore, K.N. Sood, Rashmi, D.K. Suri, M. Kar, A. Basu, R.K. Sharma, G. Bose, S. Chandra, in *Physics of Semiconductor Devices (IWPSD-2003)*, vol. 12, ed. by K.N. Bhat, A. DasGupta (Narosa Publishing House, New Delhi, 2003), 298 pp
11. H. Bahadur, R. Kishore, K.N. Sood, Rashmi, R.K. Sharma, A. Basu, D. Haranath, H. Chander, S. Chandra, in *Proceedings of 18th European Frequency and Time Forum*, Univ. Surrey, Guildford, UK, Institute of Electrical Engineers (IEE) vol. 18 (2004)
12. H. Bahadur, A.K. Srivastava, R. Kishore, Rashmi, S. Chandra, in *Proceedings 2004 14th IEEE International Symposium on Applications of Ferroelectrics*, 185 pp (2004), IEEE Catalog # 0-7803-8414-8/04/\$20.00©2004
13. H. Bahadur, S.B. Samanta, A.K. Srivastava, K.N. Sood, R. Kishore, R.K. Sharma, A. Basu, Rashmi, M. Kar, P. Pal, V. Bhatt, S. Chandra, *J. Mater. Sci.* **41**, 7562 (2006)
14. H. Bahadur, A.K. Srivastava, S.C. Garg, P. Pal, S. Chandra, in *Proc. IEEE International Frequency Control Symposium and Exhibition* **146**, IEEE ISBN 0-7803-9053-9 Catalog # 05CH37664C, 146 pp (2005)
15. H. Bahadur, A.K. Srivastava, D. Haranath, H. Chander, A. Basu, S.B. Samanta, K.N. Sood, R. Kishore, R.K. Sharma, Rashmi, V. Bhatt, P. Pal, S. Chandra, *Indian J. Pure Appl. Phys.* **45**, 395 (2007)
16. D. Dyrssen, P. Lumme, *Acta. Chem. Scand.* **16**, 1785 (1962)
17. G. Biedermann, L. Ciavatta, *Acta. Chem. Scand.* **16**, 2221 (1962)
18. D.D. Perrin, *J. Chem. Soc.* **4500** (1962)
19. F.A. Cotton, G. Wilkinson, *Advanced Inorganic Chemistry* (John Wiley & Sons Inc., New York, 1975)
20. H. Bahadur, Rashmi, R.K. Sharma, A.K. Srivastava, S. Singh, K.N. Sood, A. Basu, R. Singh, V. Bhatt, Sudhir, Paper ID: conf116a624 (Sym. J) International Conference on Materials for Advanced Technologies (ICMAT-2007) at Singapore, July 1–6 (2007)
21. B.D. Cullity, *Elements of X-Ray Diffraction* (Adison-Wesley, London, 1959)